CENTER FOR TOKAMAK TRANSIENTS SIMULATION

CTTS Overview

Stephen C. Jardin

SciDAC-4 PI Meeting

Hilton Washington DC/Rockville July 23-24, 2018

CTTS Participants

PHYSICS TEAM

- **PPPL**: J. Breslau, N. Ferraro, S. Jardin, I. Krebs
- **GA**: L. Lao, B. Lyons, P. Parks, C. Kim
- **U. Wisc**: C. Sovinec, P. Zhu
- **Utah State U**: E. Held
- **Tech X:** J. King, S. Kruger
- **SBU:** R. Samulyak
- **HRS Fusion**: H. Strauss

HPC TEAM

- **RPI**: M. Shephard, S. Seol, W. Tobin
- **LBL:** X. Li, S. Williams
- **PPPL**: J. Chen
- **SBU**: R. Samulyak

Illustrated is a typical disruption in a high-power tokamak.

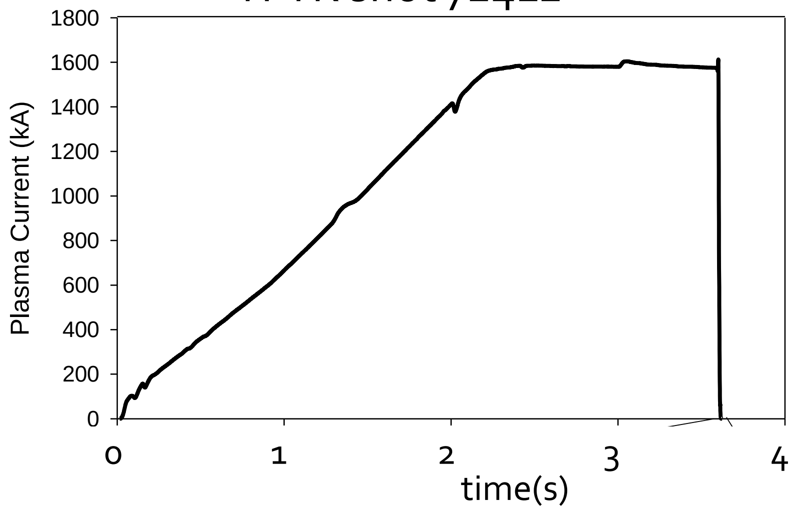

Cut of current density in simulation of disruption in NSTX shot 129922

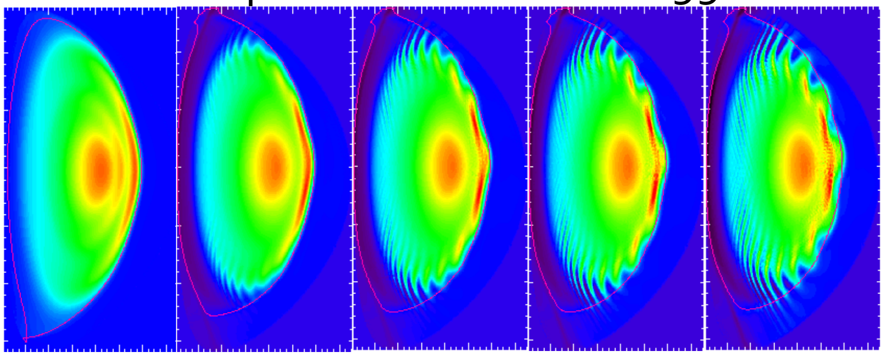

Time →

- Plasma current can decay at a rate of up to 1 MA / msec
- Large currents transferred to surrounding structures with accompanying large *forces* which *rotate*
- Sudden dump of plasma stored energy to walls and divertor plates cause *unacceptable erosion*
- Large collimated beam of multi-MeV (*runaway*) electrons can be produced which will damage vessel when they are lost

Barely acceptable in ITER, <u>NOT</u> acceptable in a Fusion Power Plant

Three major thrust areas

- Better understanding of how and why tokamaks disrupt

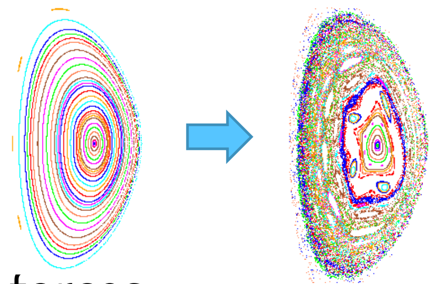

Surfaces destroyed by instability caused by excessive heating

- Quantitative prediction of the forces and heat loads due to a (worst case) disruption

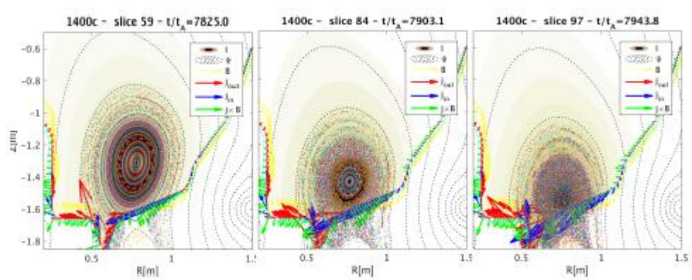

Late stages of a NSTX disruption showing forces induced in vacuum vessel

- Quantitative prediction of mitigation techniques for minimizing effects of disruption

Right is impurity injection diagram for disruption mitigation in ITER

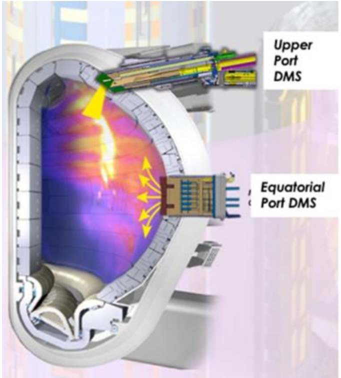

CTTS HPC Codes

Global Macroscopic Equilibrium and Stability

Localized Ablation of Impurity Pellets

NIMROD

Frontier

M3D-C1

Lagrangian Particle

An out-year goal is to tightly couple one or more from each group

Having 2 codes in each group allows code-benchmarking, especially important when new features are added

3D Resistive MHD Equations in M3D-C1 and NIMROD

$$\frac{\partial n}{\partial t} + \nabla \bullet (n\mathbf{V}) = \nabla \bullet D_n \nabla n + S_n$$

$$\left.\begin{aligned} \frac{\partial \mathbf{A}}{\partial t} &= -\mathbf{E} - \nabla\Phi \\ \nabla_\perp \bullet \frac{1}{R^2}\nabla\Phi &= -\nabla_\perp \bullet \frac{1}{R^2}\mathbf{E} \\ \mathbf{B} &= \nabla \times \mathbf{A} \end{aligned}\right\} \text{M3D-C1} \qquad \left.\begin{aligned} \frac{\partial \mathbf{B}}{\partial t} &= -\nabla \times \mathbf{E} \\ \nabla \bullet \mathbf{B} &= 0 \end{aligned}\right\} \text{NIMROD}$$

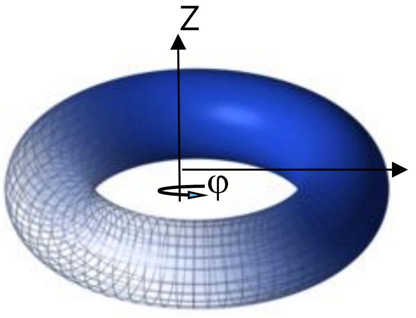

$$nM_i\left(\frac{\partial \mathbf{V}}{\partial t} + \mathbf{V} \bullet \nabla \mathbf{V}\right) + \nabla p = \mathbf{J} \times \mathbf{B} - \nabla \bullet \mathbf{\Pi}_i + \mathbf{S}_m, \qquad \mathbf{E} + \mathbf{V} \times \mathbf{B} = \eta \mathbf{J} + \mathbf{S}_{CD}$$

$$\frac{3}{2}\left[\frac{\partial p_e}{\partial t} + \nabla \bullet \left(p_e \mathbf{V}\right)\right] = -p_e \nabla \bullet \mathbf{V} + \mathbf{J} \bullet \mathbf{E} - \nabla \bullet \mathbf{q}_e + Q_\Delta + S_{eE} \qquad \mathbf{q}_{e,i} = -\kappa_{e,i} \nabla T_{e,i} - \kappa_{\parallel e,i} \nabla_\parallel T_{e,i}$$

$$\frac{3}{2}\left[\frac{\partial p_i}{\partial t} + \nabla \bullet \left(p_i \mathbf{V}\right)\right] = -p_i \nabla \bullet \mathbf{V} - \mathbf{\Pi}_i : \nabla \mathbf{V} - \nabla \bullet \mathbf{q}_i - Q_\Delta + S_{iE}$$

M3D-C1 and NIMROD have very different implementations

	M3D-C1	NIMROD
Poloidal Direction	Tri. C^1 Reduced Quintic FE	High. Order quad C^0 FE
Toroidal Direction	Hermite Cubic C^1 FE	Spectral
Magnetic Field	$\mathbf{B} = \nabla\psi \times \nabla\varphi - \nabla_\perp f' + F\nabla\varphi$	$\mathbf{B} = B_r\widehat{R} + B_z\hat{Z} + B_\varphi\widehat{\varphi}$
Velocity Field	$\mathbf{V} = R^2\nabla U \times \nabla\varphi + \omega R^2\nabla\varphi + R^{-2}\nabla_\perp\chi$	$\mathbf{V} = V_r\widehat{R} + V_z\hat{Z} + V_\varphi\widehat{\varphi}$
Coupling to Conductors	same matrix	Separate matrices w interface

Both codes use:

- Split Implicit Time advance
- Block-Jacobi preconditioner based on SuperLU_DIST
- GMRES based iterative solvers
- KPRAD non-equilibrium coronal radiation package

Localized Pellet Ablation Codes

FronTier

- Grid based Eulerian code with explicit tracking of material interfaces
- 10+ years of development and use
- Not optimal for 3D SPI simulations
- Not optimal for coupling to MHD codes

Lagrangian Pellet Code

- Based on new Lagrangian particle method(avoids SPH kernels)
- Highly adaptive, stable, convergent
- Runs much faster than FronTier in 3D with same resolution

density

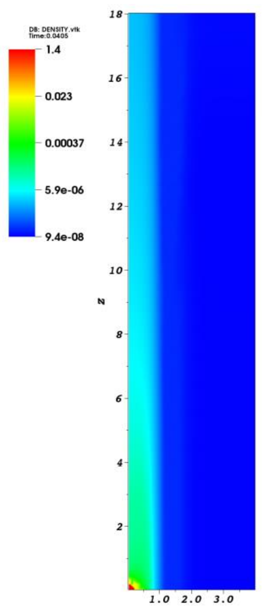

temperature

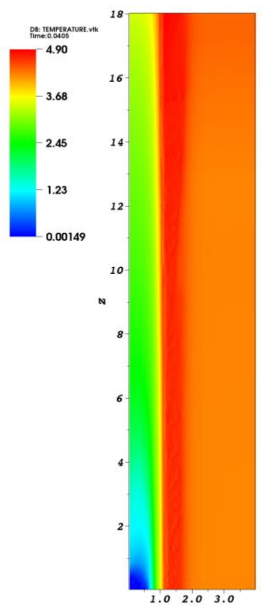

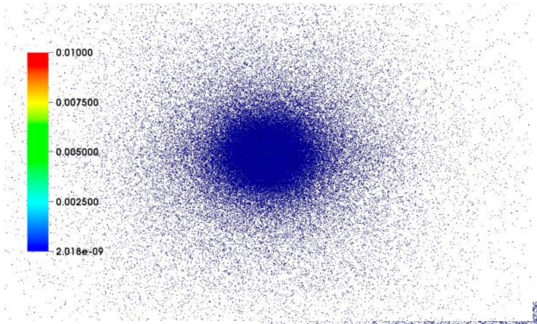

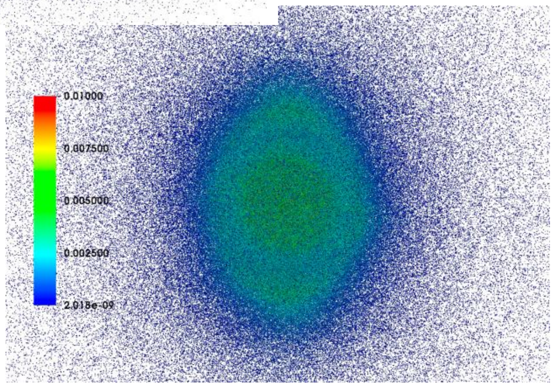

CTTS Recent CS Highlights (focus on KNL)

- M3D-C1 was part of the NESAP program with NERSC and Intel
  - 3 x speedup for matrix assembly phase
  - OpenMP implemented for top-level loop of matrix assembly
- Collaboration with SCOREC & FASTMATH on solver speedup
  - Optimizing solver parameters let to 5 x speedup for largest problems

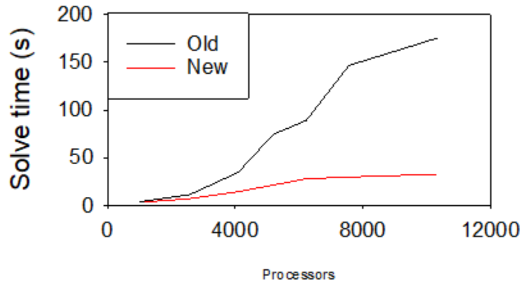

- NIMROD FASTMATH collaboration led to 40% SuperLU_DIST perf. gain
  - Biggest improvement came from use of new Synchronization-avoiding sparse triangular solve capability (trisolve) not yet released
- Also implemented OpenMP for matrix assembly

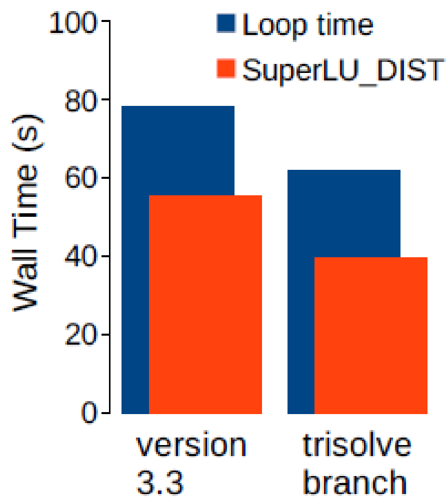

Future Directions for Solver Improvement

M3D-C1

- Make use of new SuperLU Trisolve branch in M3D-C1
- Make use of Communication-Avoiding 3D sparse LU
- Physics based reordering of unknowns
- Develop preconditioner with greater toroidal coupling
- Mixed MPI/OpenMP version of PETSc ?

NIMROD

- Make use of Communication-Avoiding 3D sparse LU
- Exploring Array Reordering to improve vectorization
- Modifying algorithm to produce symmetric matrices
  - GMRES → CG (Galerkin → Least squares)
- Use a more approximate preconditioner
- Mixed MPI/OpenMP version of PETSc?

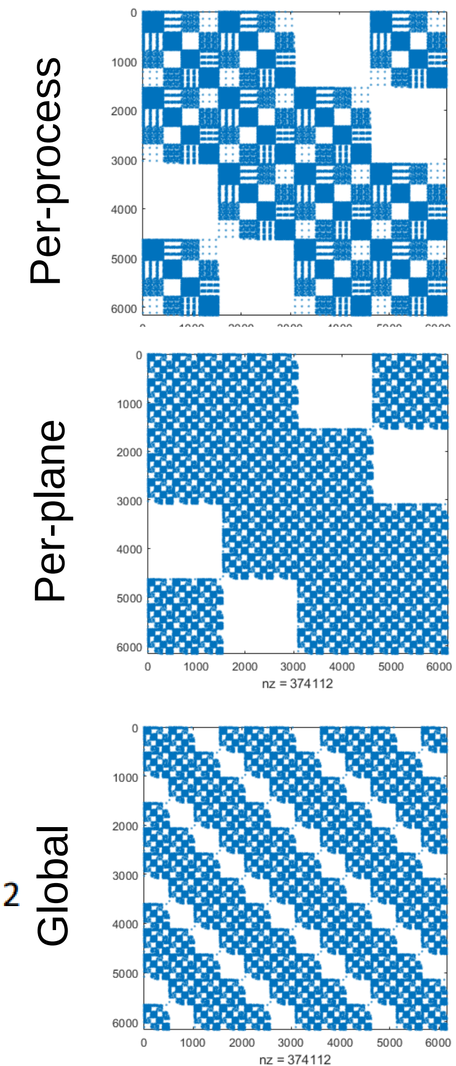

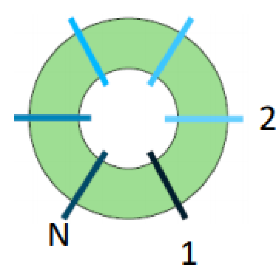

CTTS-Physics Topics

1.0 Ideal MHD Driven Disruptions
- 1.1 Prediction and Avoidance of Disruptions
- 1.2 3D Modeling of the Thermal Quench
- 1.3 3D Modeling of the Current Quench

2.0 VDEs and RWMs
- 2.1 Vertical Displacement Events
- 2.2 Resistive Wall Modes

3.0 NTMs and Mode Locking
- 3.1 Kinetic-MHD Stability of NTMs
- 3.2 Locking of NTMs in the presence of resistive walls and error fields
- 3.3 Growth of Locked Modes and how they cause disruptions

4.0 Disruption Mitigation
- 4.1 SPI Plume Model Development
- 4.2 SPI Simulations and Modeling

Emphasize code benchmarking in new regimes

CTTS-Physics Topics

1.0 Ideal MHD Driven Disruptions
- 1.1 Prediction and Avoidance of Disruptions
- 1.2 3D Modeling of the Thermal Quench
- 1.3 3D Modeling of the Current Quench

2.0 VDEs and RWMs
- 2.1 Vertical Displacement Events
- 2.2 Resistive Wall Modes

3.0 NTMs and Mode Locking
- 3.1 Kinetic-MHD Stability of NTMs
- 3.2 Locking of NTMs in the presence of resistive walls and error fields
- 3.3 Growth of Locked Modes and how they cause disruptions

4.0 Disruption Mitigation
- 4.1 SPI Plume Model Development
- 4.2 SPI Simulations and Modeling

Emphasize code benchmarking in new regimes

2.1 Vertical Displacement Events

- Both NIMROD and M3D-C1 can now simulate VDEs with a resistive wall in both 2D and 3D and calculate wall forces
- Our initial emphasis is to perform benchmark calculations in both 2D and 3D, primarily for code validation … also with JOREK
- We are also validating results as much as possible with DIII-D data

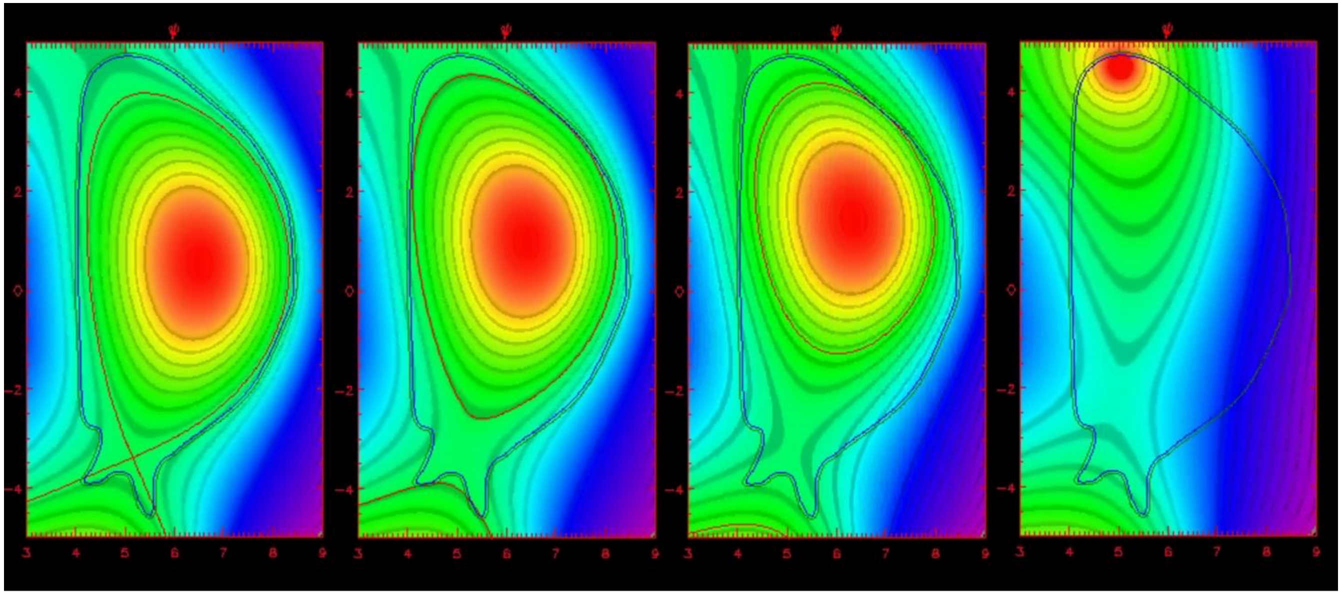

Equilibrium Wall contact Start TQ Final

VDE can occur when position control system fails, causing discharge to move up or down and contact wall

5.3 T 15MA ITER

Typical result for a M3D-C1 3D VDE Simulation of NSTX

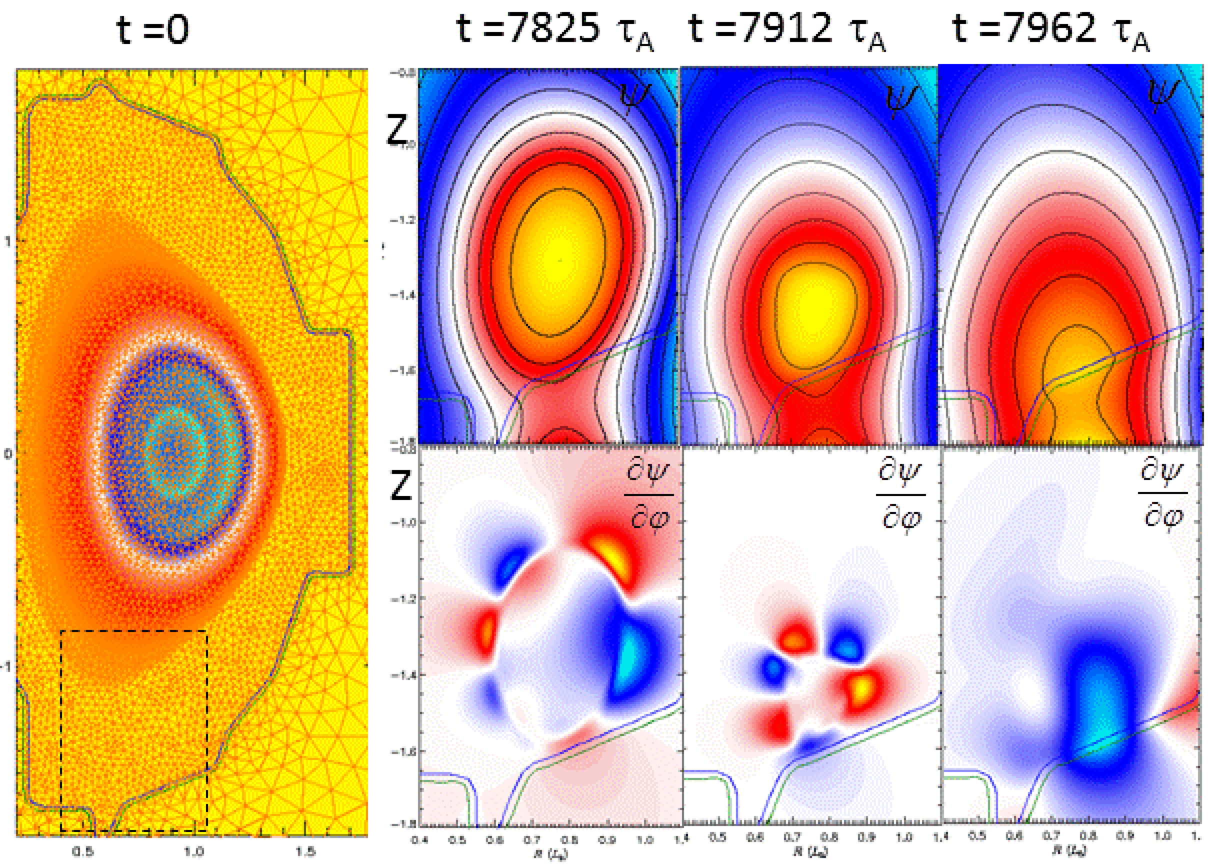

- We presently don't have any 3D benchmarks because no 2 codes have modeled the exact same case

NIMROD recently aquired the capability of 3D VDE simulations by adding a wall region

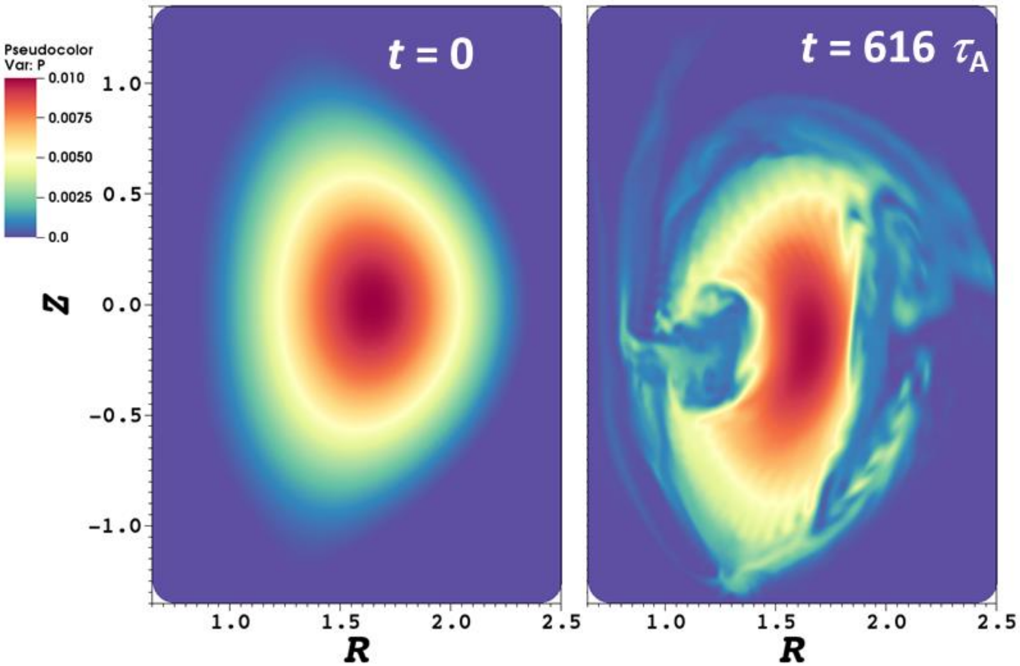

Initial and distorted plasma pressure profiles from NIMROD simulation of an asymmetric vertical displacement event (AVDE); internal region shown.

Separate external domain used during the magnetic-field advance. Implicitly coupled through an interface

FMGMRES with two complementary block-based preconditioners to solve coupled field advance.

VDE benchmark between M3D-C1, NIMROD & JOREK

Equilibrium poloidal magnetic flux

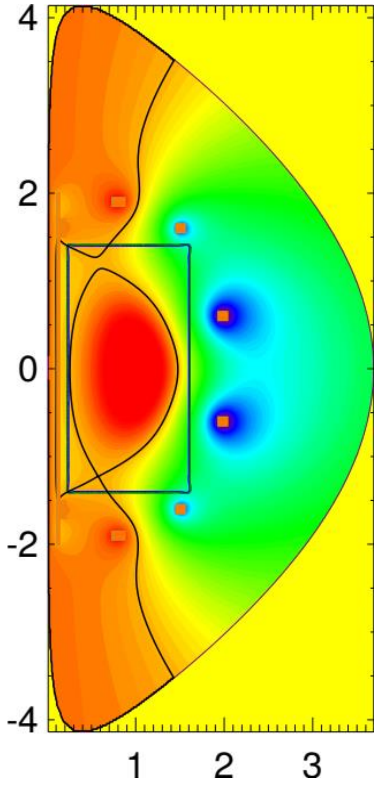

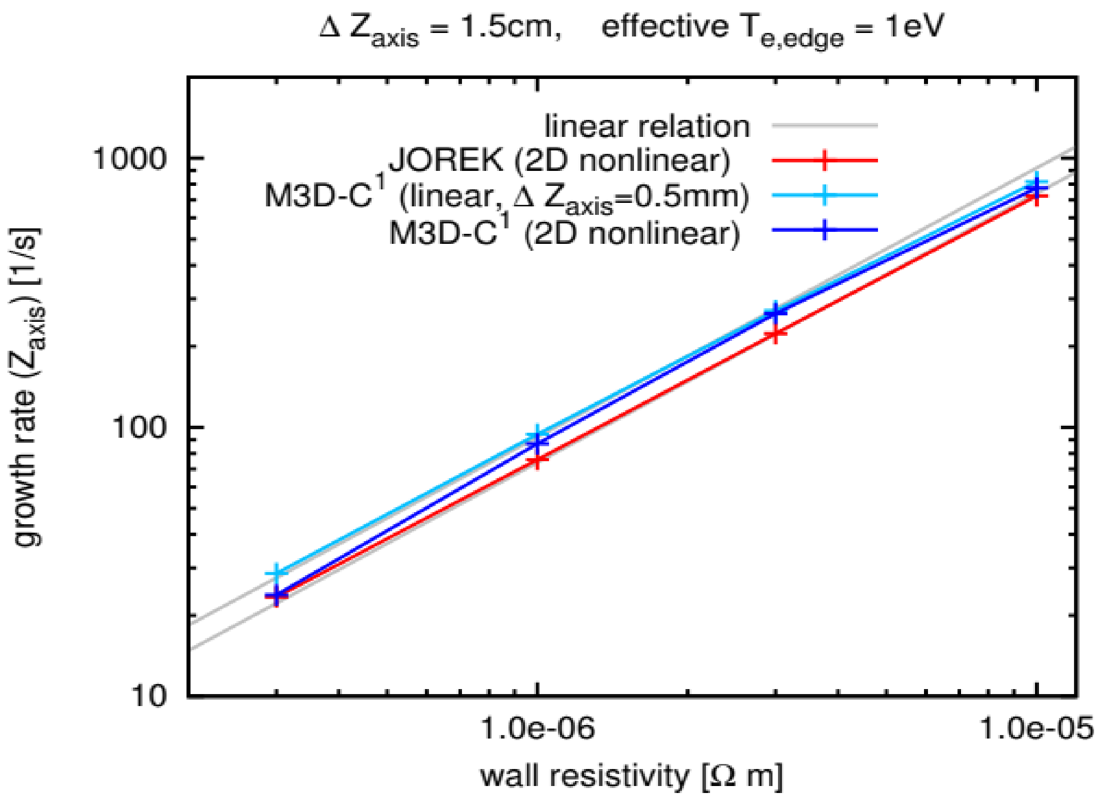

Realistic equilibrium but simplified geometry that all codes can handle. Initial comparison is 2D linear. Codes agree to within 20% on growth rates over wide range

CTTS-Physics Topics

1.0 Ideal MHD Driven Disruptions
- 1.1 Prediction and Avoidance of Disruptions
- 1.2 3D Modeling of the Thermal Quench
- 1.3 3D Modeling of the Current Quench

2.0 VDEs and RWMs
- 2.1 Vertical Displacement Events
- 2.2 Resistive Wall Modes

3.0 NTMs and Mode Locking
- 3.1 Kinetic-MHD Stability of NTMs
- 3.2 Locking of NTMs in the presence of resistive walls and error fields
- 3.3 Growth of Locked Modes and how they cause disruptions

4.0 Disruption Mitigation
- 4.1 SPI Plume Model Development
- **4.2 SPI Simulations and Modeling**

Emphasize code benchmarking in new regimes

4.1 Plume Model Development

- Kinetic model for the interaction of hot electrons with ablated gas

- Explicitly tracked pellet surface
- Phase transition (ablation model)

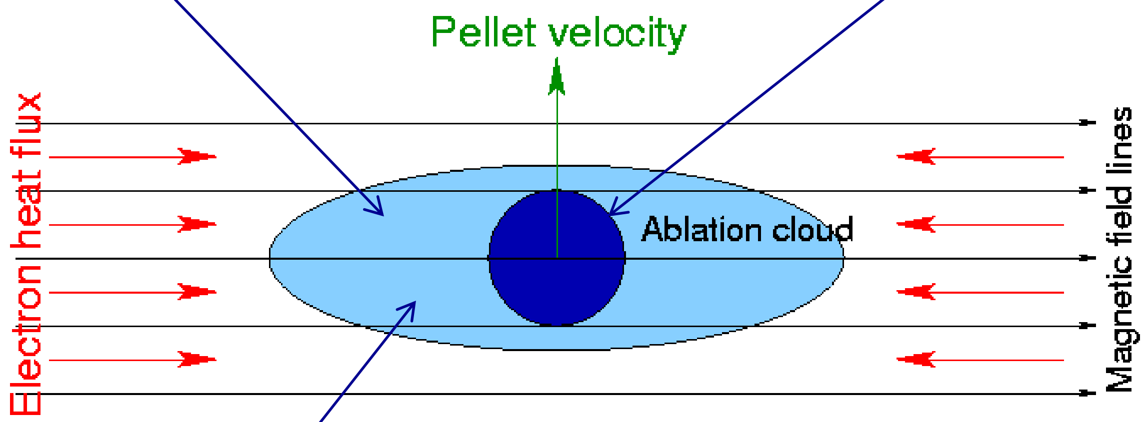

- Low Magnetic Re MHD equations
- Equation of state with atomic processes
- Radiation model
- Electric conductivity model

3D MHD Lagrangian Particle Simulations: evolution of ablation channel

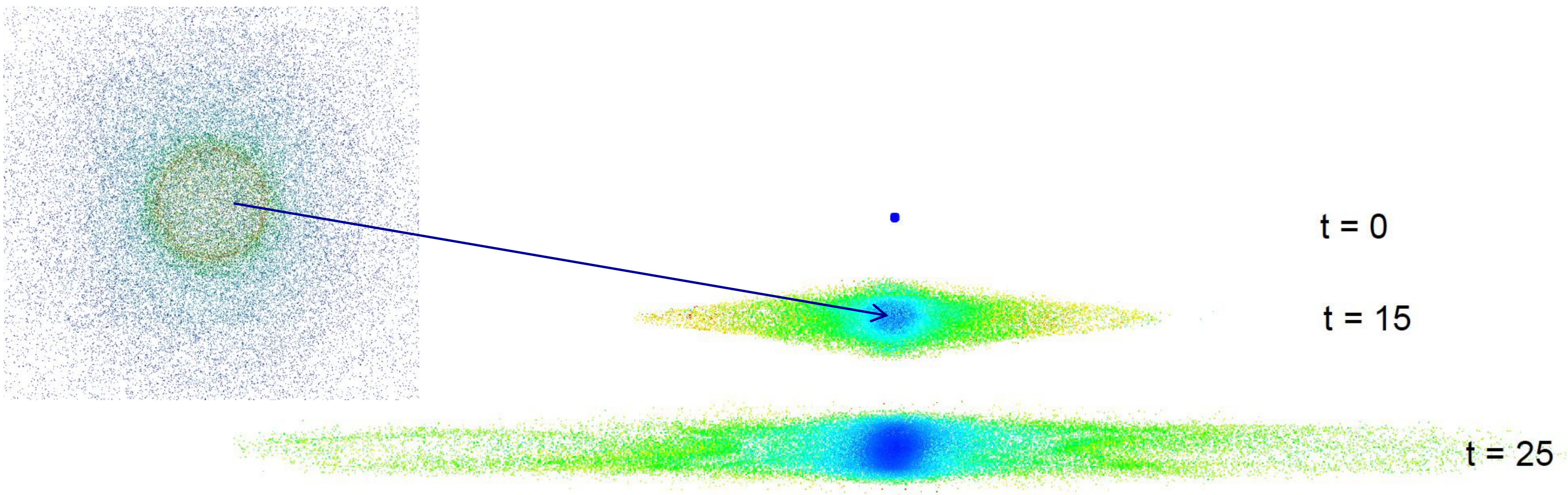

- MHD simulation of the formation and evolution of a pellet ablation cloud in 6T magnetic field
- Distributions of the ablated material are shown at the initial time (top image), at 15 μs (middle image), and 25 μs (bottom image)
- The background electron density is linearly ramped-up to its maximum value over the first 10 μs, modeling the plasma pedestal
- Ablation rate is ~ 30 g/s

3D simulations of SPI (multiple pellets) using Lagrangian particle code

- Left image: distribution of the line density integral for the kinetic heating model
- Right image: ablation flow in the vicinity of two fragments
- Reduction of the ablation rate due to the partial screening of ablation clouds is currently being investigated

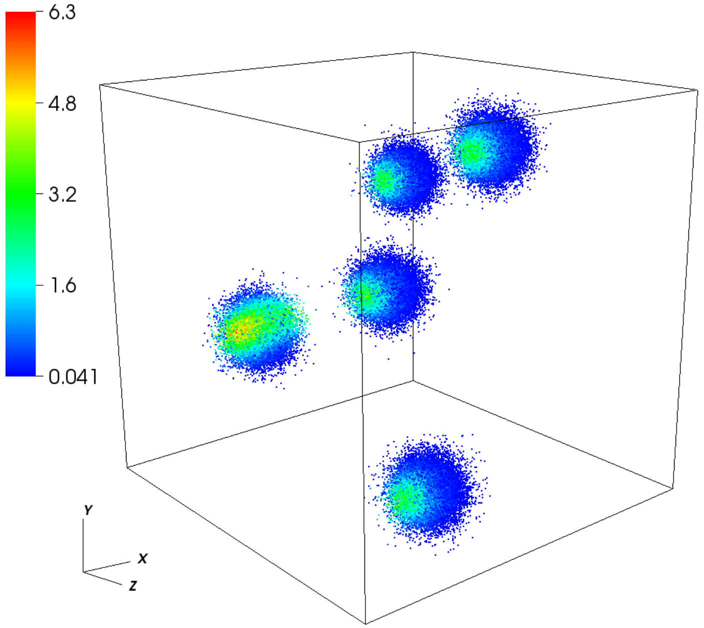

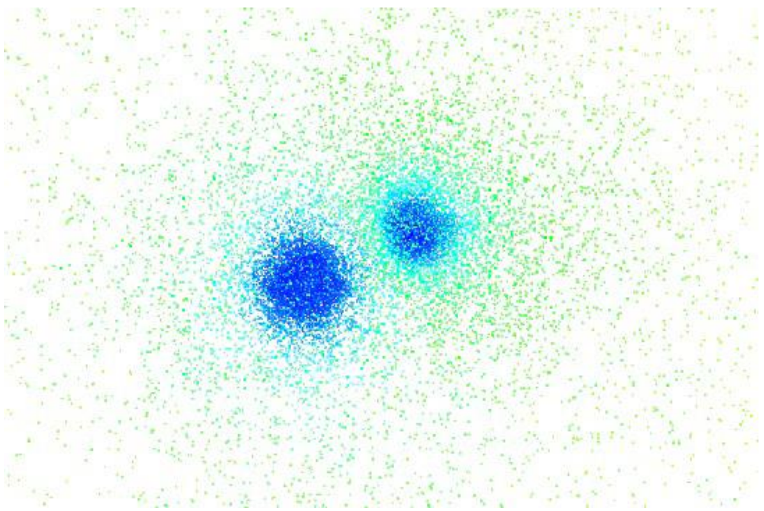

CTTS-Physics Topics

1.0 Ideal MHD Driven Disruptions
- 1.1 Prediction and Avoidance of Disruptions
- 1.2 3D Modeling of the Thermal Quench
- 1.3 3D Modeling of the Current Quench

2.0 VDEs and RWMs
- 2.1 Vertical Displacement Events
- 2.2 Resistive Wall Modes

3.0 NTMs and Mode Locking
- 3.1 Kinetic-MHD Stability of NTMs
- 3.2 Locking of NTMs in the presence of resistive walls and error fields
- 3.3 Growth of Locked Modes and how they cause disruptions

4.0 Disruption Mitigation
- 4.1 SPI Plume Model Development
- 4.2 SPI Simulations and Modeling

Emphasize code benchmarking in new regimes

4.2 SPI Simulation and Modeling

Both NIMROD and M3D-C1 have impurity pellet and radiation models to model Shattered Pellet Injection (SPI) mitigation experiments on DIII-D and ITER

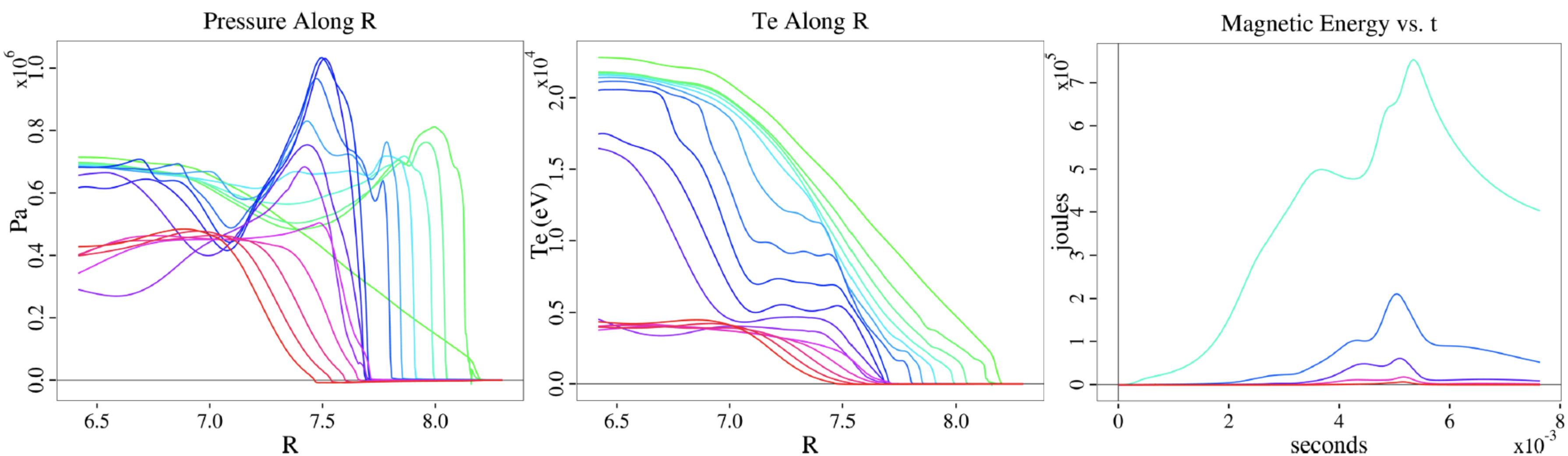

- NIMROD ITER simulation of pellets being injected at time t=0
- P and Te profiles, Δt=0.5 ms along radial midplane chord from center to wall

Codes have the capabilities but have not yet been fully benchmarked

Successful axisymmetric benchmark between M3D-C1 and NIMROD's impurity coupling

- BENCHMARK DETAILS
  - 2D, nonlinear, single-fluid
  - KPRAD for ionization & radiation
  - On-axis Gaussian source of neutral argon
  - Constant diffusivities and main ion density
- EXCELLENT AGREEMENT BETWEEN CODES
  - Thermal-energy evolution
  - Loss power, mainly line radiation & ionization

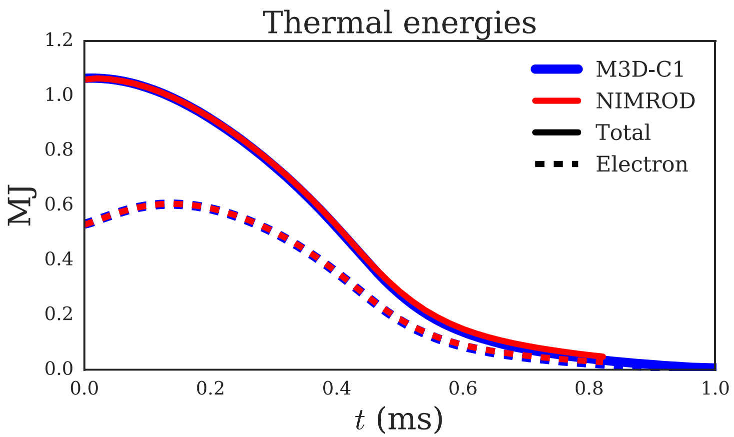

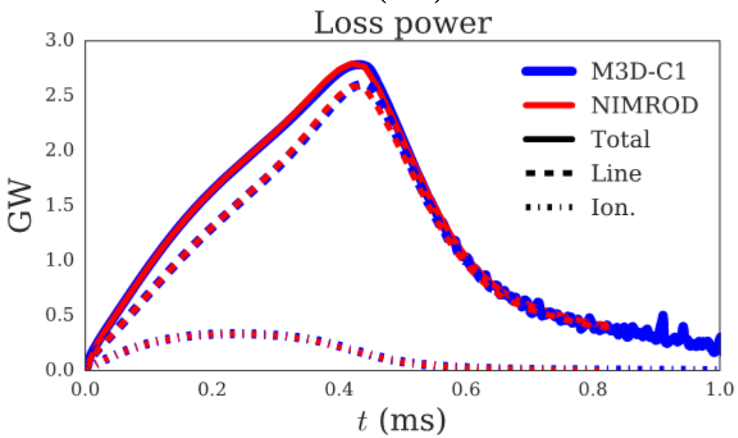

- Benchmarking now moving to 3D phase with pellets
- Later stage will incorporate pellet model from Frontier or LPM

THANK YOU!

Extra slides

Chapman-Enskog-like (CEL) closures in NIMROD

Picard and Newton methods implemented for simultaneous, nonlinear T and perturbed particle distribution advance.

Electron kinetic heat flow response (top) and perturbed particle distribution contours (bottom) after T has flattened across a slab island.

Implementing parallelization over speed grid points to improve efficiency of matrix/vector computations.

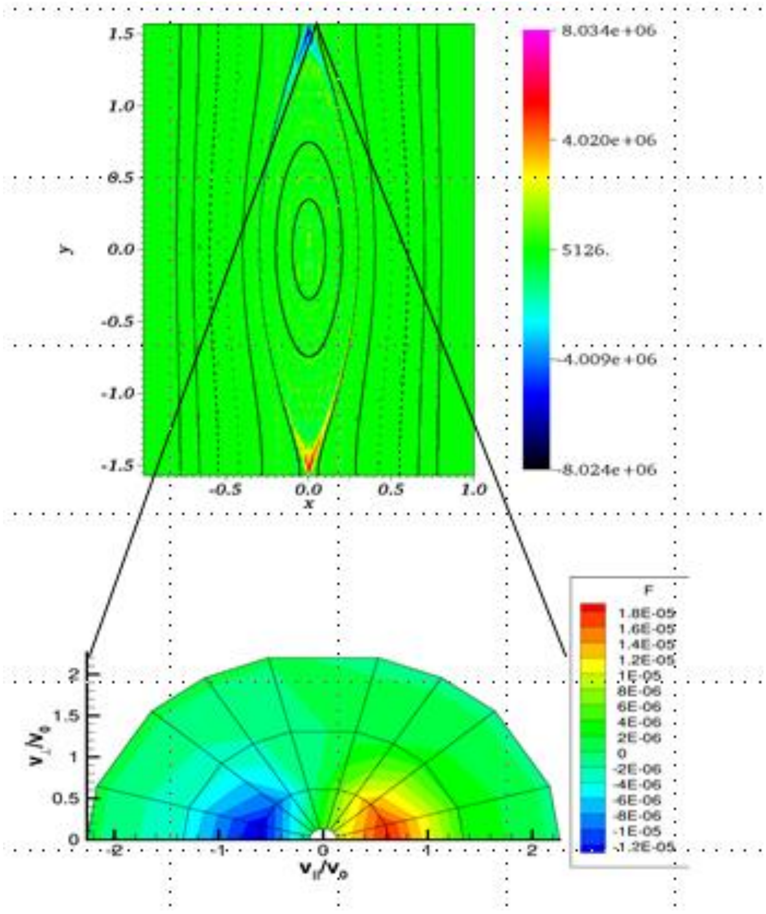

Global Pellet ablation code: ideas for coupling with NIMROD / M3D-C1:

- Lagrangian particle approach is very promising for coupling with global tokamak codes:
    - No need for overlapping domain decomposition typical for grid-based codes
    - No artificial plasma background is present in LP simulations – only ablated material is evolved. Easy to extract ablation flow data.

- Stage 1: loose coupling. Pre-compute pellet / SPI ablation data and use them as source terms in global MHD codes

- Stage 2: Strong coupling

    - Global MHD and Pellet codes are linked and run in parallel on a supercomputer using different nodes / communicators (a light version of LP code will be used – stripped of all functions not relevant to the pellet ablation model).
        - LP pellet code can be implemented based on the current PIC module in NIMROD

    - Data exchange is performed at the time step of the global MHD code

    - Pellet code data is represented in terms of basis functions of the global code and corresponding coefficients are sent to the global MHD code

Progress on 2D nonlinear simulations of VDE in ITER

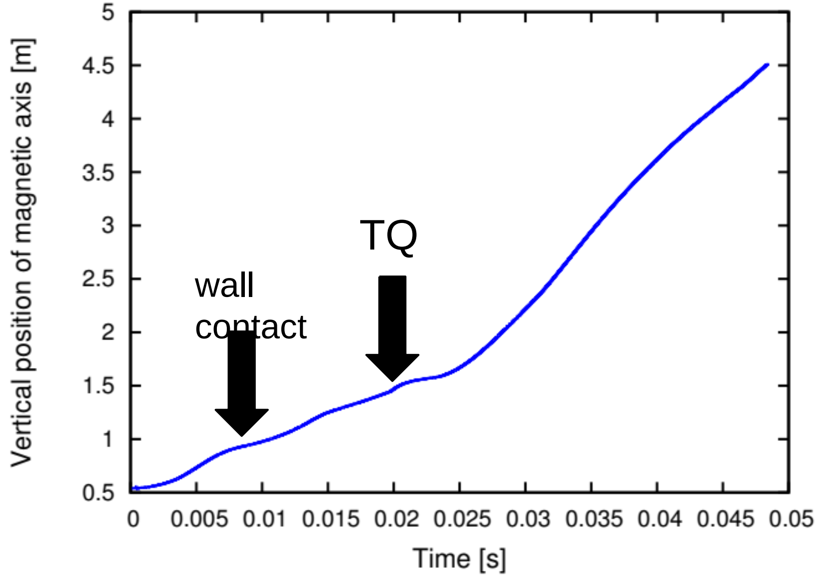

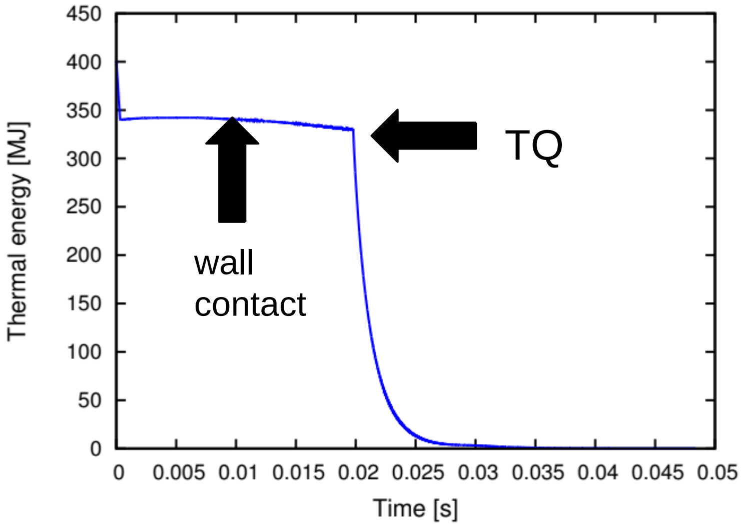

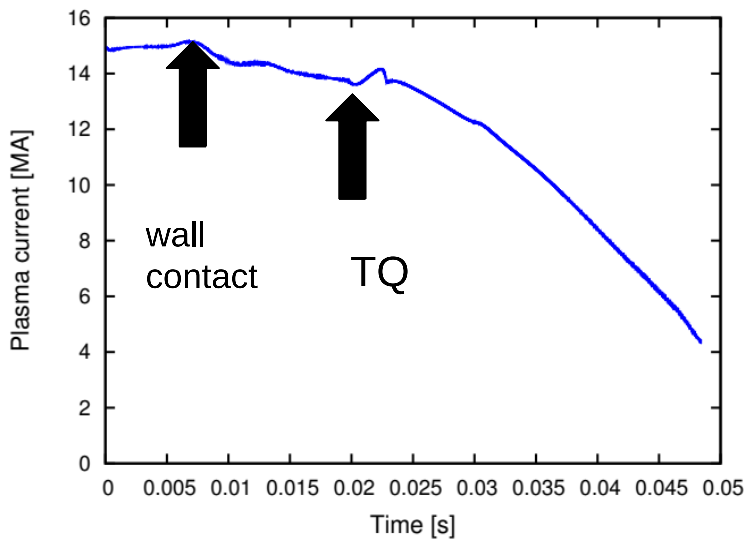

- Artificial TQ initiated by increasing perpendicular heat diffusion by factor 1000

M3D-C1 Mesh Related Developments

- Support of alternative ordering of unknowns
  - By node ordering (all dof at first node, followed by all dof at second node, etc.) not ideal for numerical conditioning when the nodal dof list has derivative dof – M3D-C1 has value, 1st and 2nd derivative dof.
  - Developing support for by component ordering – all dof for the first component are followed by all dof of the second component, etc.
- Improved solver interface toward full thread safe assembly
- Support of PIC capability being added to M3D-C1
  - Developing a general components for distributed mesh PIC methods
  - PUMI based heavy overlap and adjacency based element containment being used in M3d-C1 with PIC
- Extensions to geometry/meshing
  - More flexible options for defining mesh regions used for applying resistive wall boundary condition

M3D-C1 By Component DOF Ordering

- Developing a procedure to support the by component dof ordering
  - Support ordering for the nodes at the
    - process level,
    - poloidal plain level, or
    - globally
  - Alternatives options
    - Yield different matrix sparsity patterns
    - Support different preconditioning options
    - Have very different assembly interprocess communication requirements
    - Likely to yield different solution time
  - Implementation is generic – will allow the effective evaluation of the options

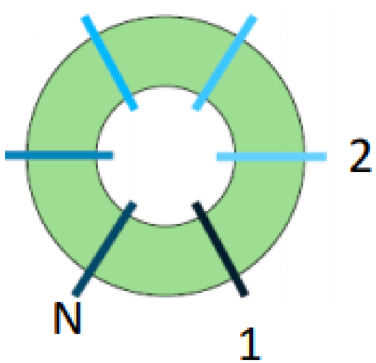

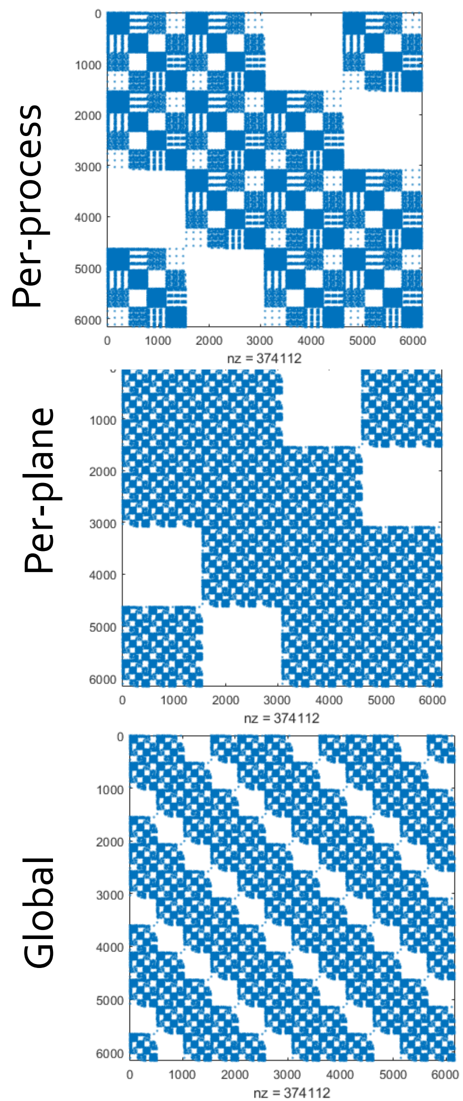

M3D-C1 Linear Solver Interface

- Need more efficient linear system assembly step
- As a first step: Implemented a generic linear solver interface (LAS) to wrap multiple supporting linear algebra libraries
  - Compile-time decision to target a specific backend library
    - Allows leveraging of best library/implementation for a target machine without touching matrix assembly algorithms
    - Libraries for accelerators (CUDA / PHIs)
    - Libraries for threaded or MPI-only
  - LAS API is aggressively inlined to compile down to identical machine code as raw use of a library backend
  - Currently supports
    - cuSparse (CUDA)
    - PETSc
- Next: Implement PUMI-based finite element assembly routines using LAS interfaces

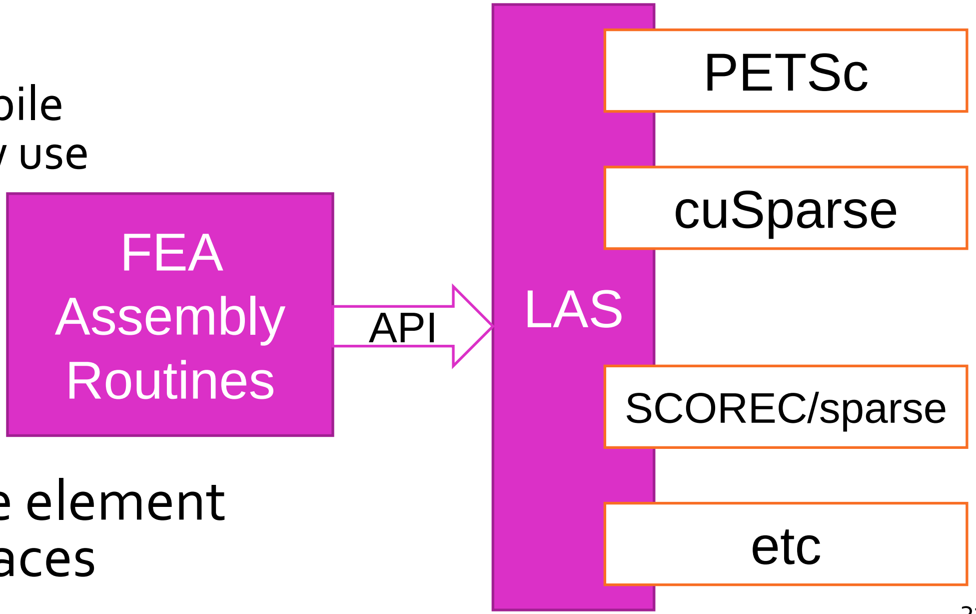

Parallel Unstructured Mesh PIC – PUMIpic

- PUMIpic – Components to support PIC operations on distributed unstructured meshes (2D and 3D)
  - Mesh centric – mesh is distributed, particles
    mesh – no independent particle structure, p
    better memory access
  - Distributed PUMI mesh with large overlap (avoid communication during a push)
  - Particle migration and load balancing
  - Adjacency-based particle containment determination
  - Mesh-to-Particle and Particle-to-Mesh field transfers
  - Coordination of parallel continuum solve

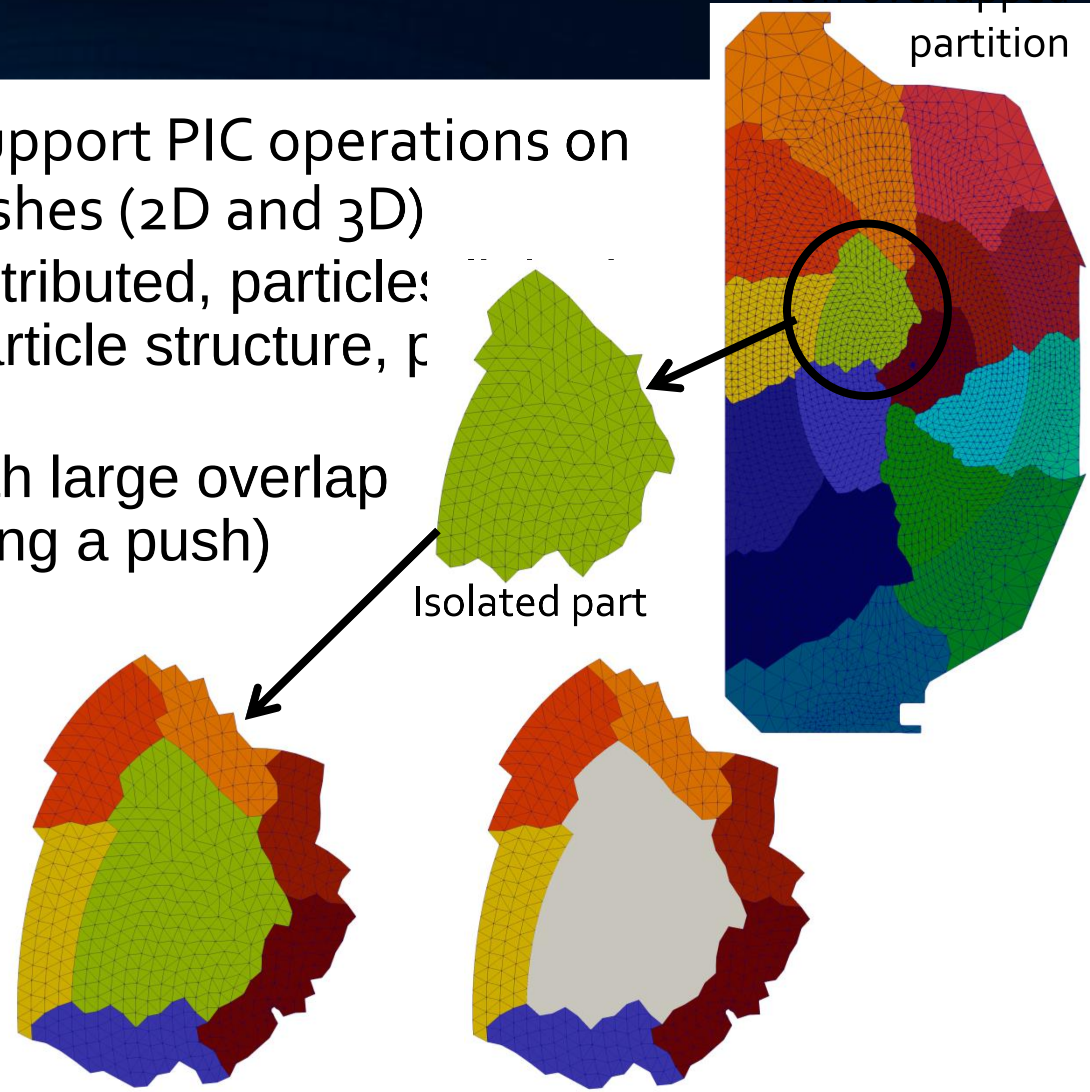

Ablation model for Ne-D2 pellets implemented in M3D-C1

- Practical, analytic expression fit to more complex ablation model (Parks)

$$G\,(\mathrm{g/s}) = \lambda(X)\left(\frac{T_e}{2000\ \mathrm{eV}}\right)^{5/3}\left(\frac{r_p}{0.2\ \mathrm{cm}}\right)^{4/3}\left(\frac{n_e}{10^{14}\ \mathrm{cm}^{-3}}\right)^{1/3}$$

λ is fitting function, depending on molar fraction of D2, X

- M3D-C1 implementation
  - Advance pellet location in time
  - Calculate number of particles ablated and pellet-surface recession at each time step
  - Deposit main ion and/or impurities onto arbitrary spatial distribution (e.g. 2D or 3D Gaussian)

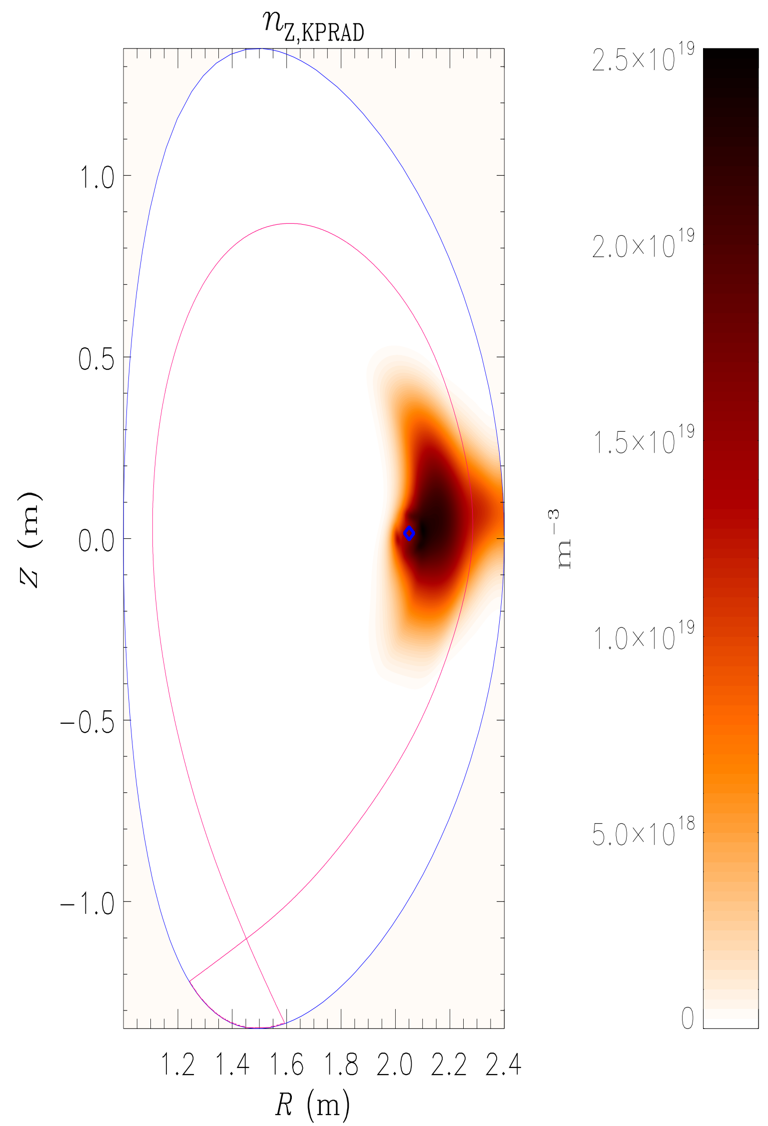

NIMROD Is Ready to Assess Viability of Shatter Pellet Injection (SPI) Successfully implemented First PiC-Based SPI Model and Tested DIII-D and ITER Simulations

- **SPI is the leading candidate for the ITER Disruption Mitigation System (DMS)**
  - **Enable deeper penetration of rear fragments by cooling of frontal segments**
- **Developed comprehensive PiC based model to mimic SPI fragment plume using an analytic mixed species pellet ablation expression and implemented in NIMROD**
  - **Discrete PiC marker represents subset of SPI plume fragments**
- **Impurity ionization, recombination, and radiation from KPRAD[1]**
- **Single-fluid resistive MHD model based on single-temperature equation**

q heat flux, Q radiation and heating, $T\sum\frac{\Delta n_\alpha}{\Delta t}$ dilution cooling (*ablation and electrons*)

$$n_{tot}\left(\frac{\partial T}{\partial t}+\mathbf{V}\cdot\nabla T\right)=(\Gamma-1)\left(-p\nabla\cdot\mathbf{V}-\nabla\cdot q+Q-\Pi:\nabla\mathbf{V}\right)-T\sum\frac{\Delta n_\alpha}{\Delta t}$$

$n_{tot}=n_i+n_e+\sum_Z n_Z$ (*impurities include neutrals*)

- **Benchmarked with M3D-C1 using 2D simplified impurity Argon source**
- **Successfully tested DIII-D and ITER SPI simulations**
  - **MHD mixing plays important role in thermal-quench dynamics**
  - **Three phases: Growth of MHD modes, thermal collapse, magnetic-surface healing**

ITER SPI DMS

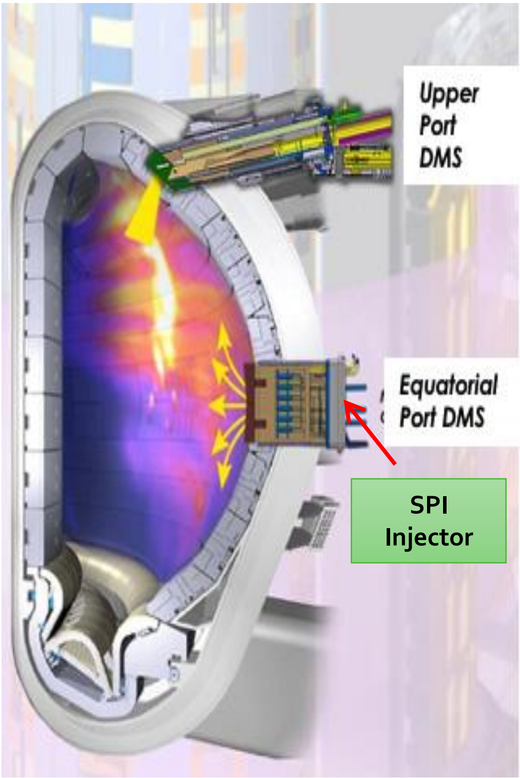

Kim APS Invited 2018

GENERAL ATOMICS

NIMROD SPI, 0.5kPa-m^3 Ne Pellet, 12.5MA Hybrid ITER Equilibrium

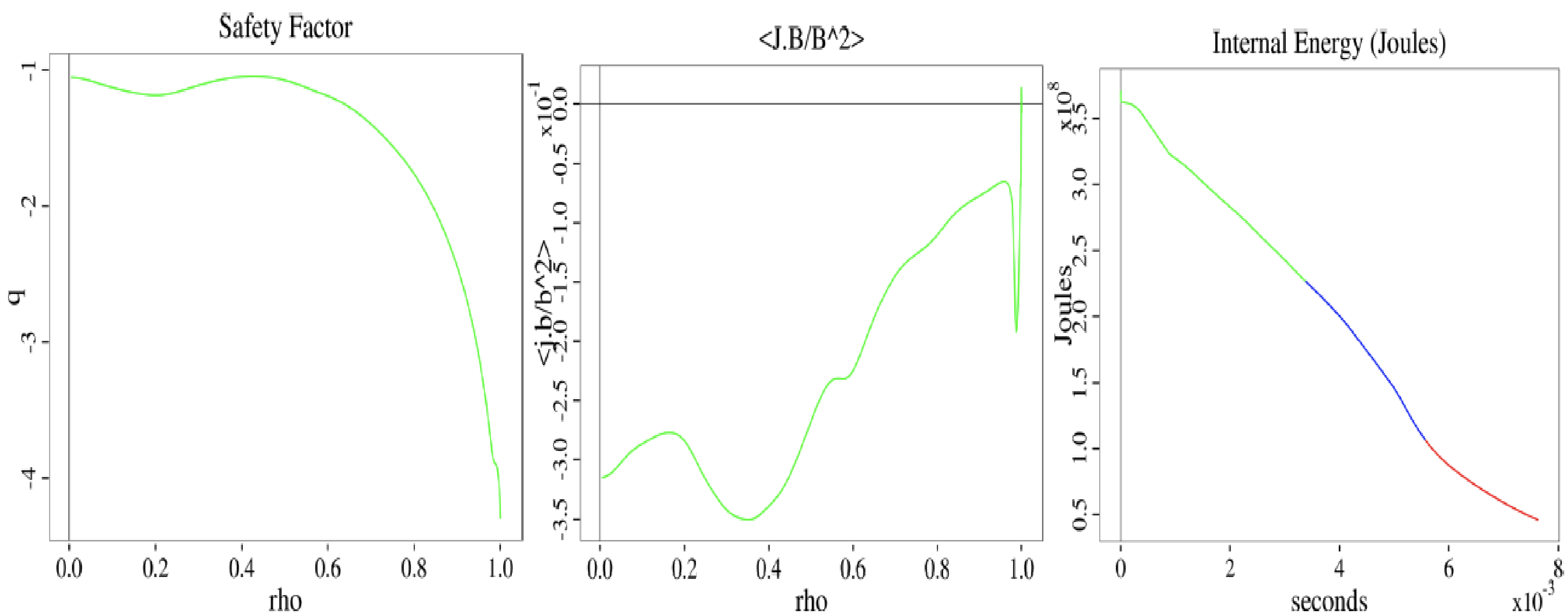

Temperature-Dependent Resistivity and Thermal Conduction

- 128x128(pd=3) n=[0,5], S$\sim 10^6$, Pr$\sim 10^5$
- 125 fragments/25 particles, r_0=1.71mm, v=500m/s, Δr_{dep}=40cm/$\Delta\phi_{dep}$=0.5$\times 2\pi$
- (48hrs + 48hrs + 48hrs) $\times$ 384 processors $\times$ 2 (premium queue) = 110khrs@NERSC[1]
- note dip in internal energy between t$\simeq$[4.0,6.0]ms

[1]N rch Scientific Computing Center, a US DOE-OFES User Facility

Radiation Peak at $t \cong [4.0, 6.0]$ms Coincides with Peak MHD Mode Activity

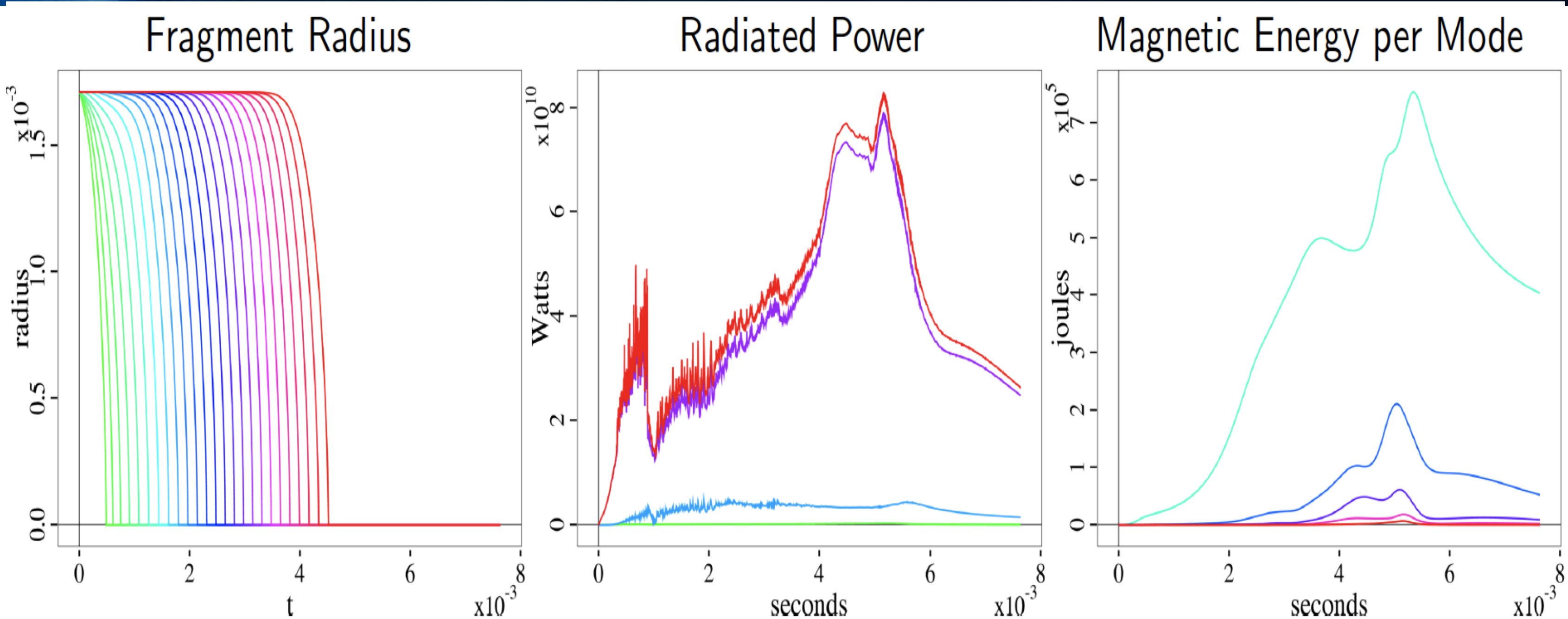

- all fragments ablate by t_{ablt}=4.5ms, sim ends at t=7.6ms, ΔThermal Energy = 318.5MJ
  - total radiated energy 317MJ = 294MJ line radiation + 22MJ recombination + 1MJ Brem.
- n=1(cyan), n=2(blue), n=3(purple), n=4(magenta), n=5(red)
  - MHD dominated by n=1 (single injector)
  - dip in mode energy coincides with t_{ablt}
  - radiation peak coincides with n=1 kink at t≃[4.0,6.0]ms

Radial Profiles Show Fast Collapse at Radiation Peak

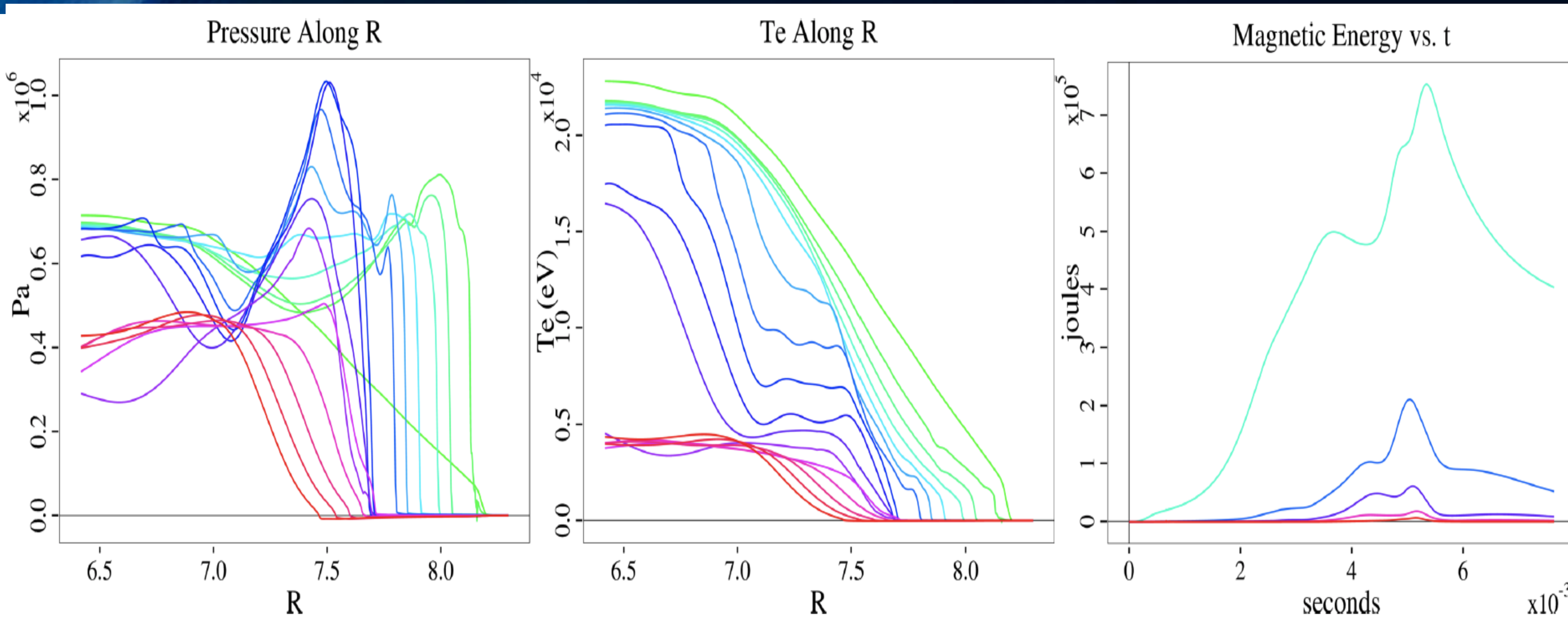

- P and T profiles, Δt=0.5ms, along radial midplane chord at ϕ=0 from axis to outer wall
- temperature pedestal (at R$\simeq$7.4m) due to (1,1) island begins forming at t=2.5ms
  - indicates early (1,1) instability
  - closer examination reveals smaller pedestals earlier in time (*see Poincare plots*)
- temperature at core collapses between t=4.5ms and t=5.0ms
  - corresponds to mode activity and radiation peak at t$\simeq$[4.0,6.0]ms
  - after collapses, remnant core ($\simeq$4keV) heals and relaxes

C. C. Kim (SLS2)

NIMROD used to simulated SPI induced TQ for ITER baseline and hybrid scenarios with varying impurity contents

Ne[kPa .m³]	Ne:D2	Ip [MA]	r_frag [mm]	S ($\times10^6$)	Kperp[m²/s]	Kpara[m²/s]	kin_vis [m²/s]	mesh	Δt [µs]	τ_{TQ} [ms]	Burnt/total
0.5	0:1	15	1.71	1.85	10	10^{10}	2×10^4	96x96	0.2	8	125/125
1	0:1	15	2.15	1.85	10^2	10^7	5×10^3	96x96	0.5	5	75/125
0.5	10:1	15	4.42	1.85	10	10^{10}	2×10^4	64x72	0.2	4.5	65/125
0.5	10:1	15	4.42	18.5	10	10^{10}	2×10^4	64x72	0.2	4.5	65/125
0.5	10:1	15	4.42	1.85	10	10^{10}	2×10^2	64x72	0.2	4.5	75/125
0.5	10:1	15	3.51	1.85	10	10^{10}	2×10^4	64x72	0.2	4.5	150/250
0.5	1.5:1	15	2.51	1.85	10^2	10^7	5×10^3	96x96	0.5	>6	125/125
0.5	0:1	12.5	1.71	1.62	10^2	10^7	5×10^3	96x96	0.5	>5	125/125

- Fixed plasma resistivity and thermal conductivity coefficients
- 25 PiC markers at V=500 m/s
- n=0-5 toroidal modes

Twice larger amount of pure neon SPI reduces TQ time by ~35% for ITER 15 MA baseline scenario

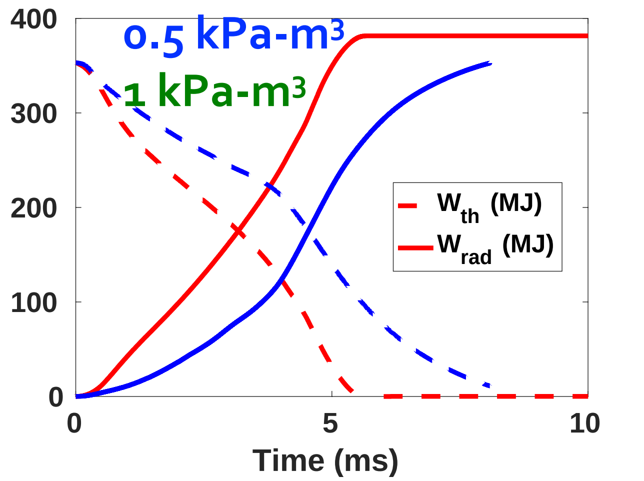

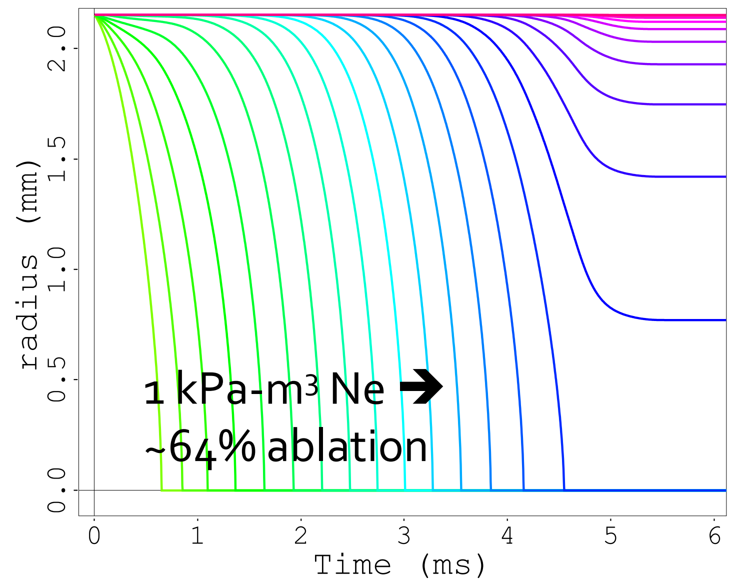

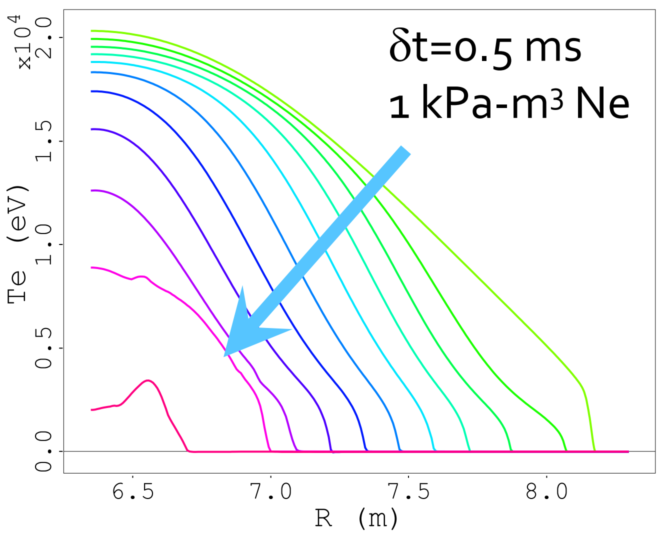

- **0.5 kPa-m³ neon →**
  - 8 ms TQ
  - 100% ablation of injected pellet during TQ
- **1 kPa-m³ neon →**
  - 5 ms TQ
  - ~64% ablation
- **TQ time traces not very sensitive to assumed plasma resistivity & viscosity**

Comparing 1-D Spherically Symmetric results for D_2 pellet (Ablation rate and sonic radius quantities)

$$g = 7/5,\ I_* = 7.5\ \text{eV},\ r_p = 2\ \text{mm},\ T_{e¥} = 2\ \text{keV},\ n_{e¥} = 10^{14}\ \text{cm}^{-3}$$

(No atomic processes included and no electrostatic shielding)

Case	G (g/s)	T_* (eV)	r_* (mm)	P_{sur}/p_*
Semi-analytic Parks*	119.1	3.5616	5.161	4.844 p_* = 27.8 bar
CAP** code	120.7	3.65	5.25	4.66
FronTier*** June 2018	119.2	3.580	5.18	5.13 p_* = 27.7 bar

*Parks, "The ablation rate of some low-Z pellets in fusion plasmas using a kinetic electron energy flux model" to be submitted to Phys Plasmas 2018

Ishizaki and Parks, Phys Plasmas **5, 1968 (2004)

***Samulyak, Lu, and Parks, Nucl Fusion **47** 103 (2007)

Comparing 1-D Spherically Symmetric results for Ne pellet with electrostatic/albedo effects

$\gamma = 5/3,\ r_p = 2\ \text{mm},\ T_{e\infty} = 2\ \text{keV},$ **(No ionization)**

$n_{e\infty} = 10^{14}\ \text{cm}^{-3}\ ,\ n_{eff} = 1.068 \times 10^{13}\ \text{cm}^{-3}$

Case	G(g/s)	T_* (eV)	p_* (bar)
Semi-analytic 2014 Parks	51.74	6.623	5.858
Semi-analytic 2018 Parks	52.86	-------	------
FronTier June 2018	53.37	-------	------

- Excellent agreement between semi-analytic and Frontier code (version 2018) without ionization processes
- Comparison with Saha ionization included is in progress